Pailoplee and Choowong *Earth, Planets and Space* 2014, **66**:8
http://www.earth-planets-space.com/content/66/1/8

Earth, Planets and Space
a SpringerOpen Journal

FULL PAPER Open Access

Earthquake frequency-magnitude distribution and fractal dimension in mainland Southeast Asia

Santi Pailoplee* and Montri Choowong

Abstract

The 2004 Sumatra and 2011 Tohoku earthquakes highlighted the need for a more accurate understanding of earthquake characteristics in both regions. In this study, both the *a* and *b* values of the frequency-magnitude distribution (FMD) and the fractal dimension (D_C) were investigated simultaneously from 13 seismic source zones recognized in mainland Southeast Asia (MLSEA). By using the completeness earthquake dataset, the calculated values of *b* and D_C were found to imply variations in seismotectonic stress. The relationships of D_C-*b* and D_C-(*a*/*b*) were investigated to categorize the level of earthquake hazards of individual seismic source zones, where the calibration curves illustrate a negative correlation between the D_C and *b* values ($D_c = 2.80 - 1.22b$) and a positive correlation between the D_C and *a*/*b* ratios ($D_c = 0.27(a/b) - 0.01$) with similar regression coefficients ($R^2 = 0.65$ to 0.68) for both regressions. According to the obtained relationships, the Hsenwi-Nanting and Red River fault zones revealed low-stress accumulations. Conversely, the Sumatra-Andaman interplate and intraslab, the Andaman Basin, and the Sumatra fault zone were defined as high-tectonic stress regions that may pose risks of generating large earthquakes in the future.

Keywords: Seismicity; Frequency-magnitude distribution; Fractal dimension; Mainland Southeast Asia

Background

Various statistical techniques assessing the seismicity, frequency-magnitude distribution (FMD; Gutenberg and Richter 1944), and fractal dimension (D_C) (Wyss et al. 2004) are regarded as effective approaches used to understand the local seismotectonic activities. Both the *b* value of the FMD and the D_C value are significantly related to, and therefore directly controlled by, the seismicity and tectonic stress levels in that region (Scholz 1968; Öncel et al. 1996). During the past few decades, the relationship between the *b* and D_C values has been successfully calibrated (Hirata 1989; Öncel and Wilson 2002; Wyss et al. 2004), and the D_C/b ratio has been used as an indicator of earthquake hazards (Bayrak and Bayrak 2012).

After the devastation caused by the M_w-9.0 earthquake on December 26, 2004, the mainland Southeast Asia (MLSEA; Figure 1) has been recognized as one of the most seismically active regions in the world. Both interplate and a number of intraplate regimes are defined as hazardous earthquake sources. More than 45 major earthquake events ($M_w \geq 7.0$) have been reported during 1962 to 2013 within the MLSEA. Accordingly, evaluation of the FMD *a*, *b*, and D_C values of all earthquake sources recognized in the MLSEA is important and is therefore the primary focus of this study. The results of this study may be useful for seismic hazard assessments for countries in the Association of Southeast Asian Nations (ASEAN).

* Correspondence: Pailoplee.S@gmail.com
Earthquake and Tectonic Geology Research Unit (EATGRU), Department of Geology, Faculty of Science, Chulalongkorn University, Bangkok 10330, Thailand

Method

Seismic sources

Present-day activities detected at the Indo-Australian and Eurasian plate collision zone have revealed that various styles of tectonic regimes contribute in various ways to the overall seismic activities occurring within MLSEA's territory. Interplate regimes dominate along the Sumatra-Andaman subduction zone, including central Myanmar, central Sumatra Island, and off the coast of the Andaman Sea, whereas an intraplate regime spreads eastward in the vicinity of eastern Myanmar, Thailand, Laos, and southern China (Pailoplee et al. 2013). To analyze seismic hazards, previous research has defined several seismic source zones in the MLSEA. For example, Nutalaya et al. (1985) and Charusiri et al. (2005) proposed 12 and 21 zones, respectively,

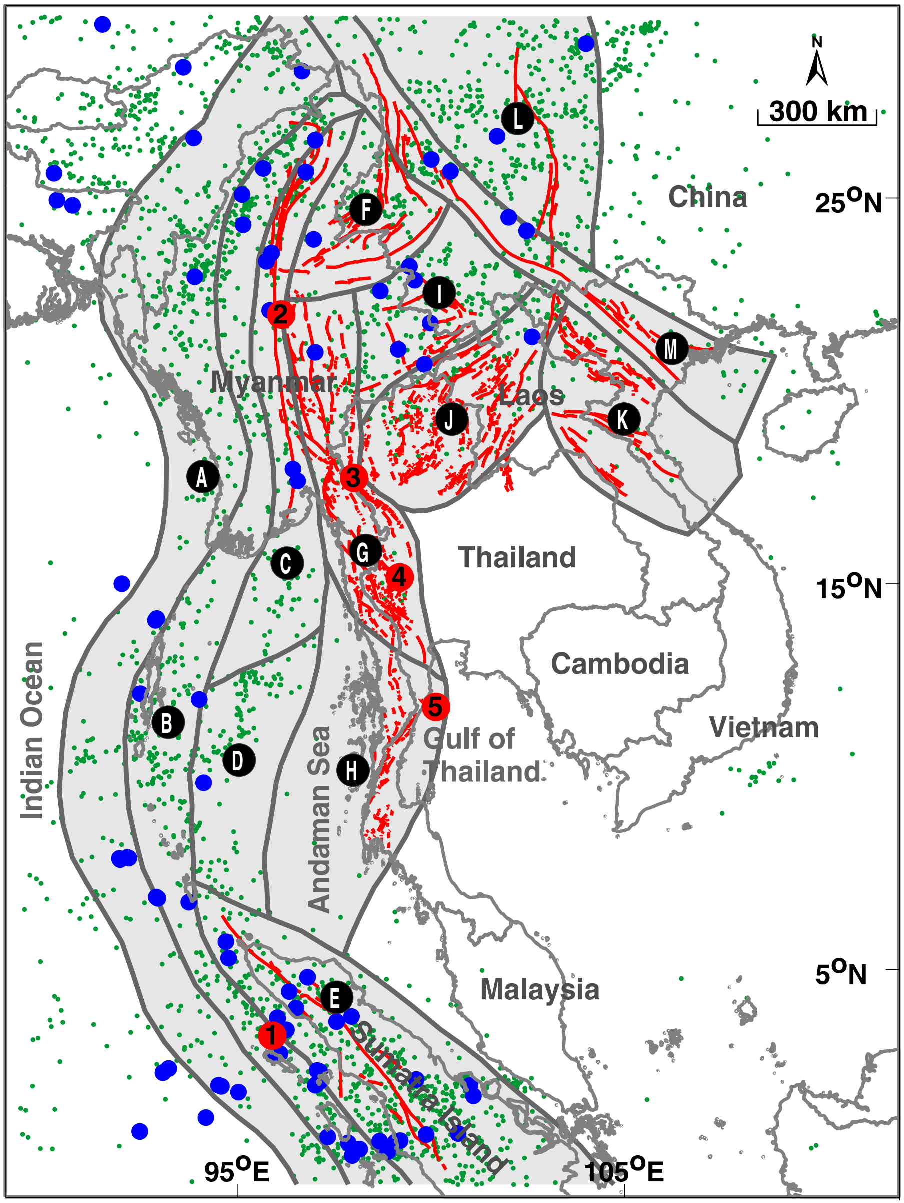

Figure 1 Map of mainland Southeast Asia (MLSEA) and the 13 designated seismic zones (A to M). The map shows epicentral distributions of completeness earthquakes with $m_b \geq 4.0$ reported during the period 1974 to 2010 (green circles), earthquakes with $m_b \geq 7.0$ (blue circles), and significant earthquakes mentioned in the text (red circles). Red lines depict the fault lines compiled by Pailoplee et al. (2009). Grey polygons indicate the geometry of the individual seismic source zones proposed by Pailoplee and Choowong (2013).

according to the various available tectonic, geological, and seismicity information. However, based on the most recent data, Pailoplee and Choowong (2013) modified the seismic source zones of both Nutalaya et al. (1985) and Charusiri et al. (2005) and proposed 13 new zones (A to M), which are used in this study (Figure 1; Table 1). The details of each zone are described briefly as follows.

The Sumatra-Andaman interplate and intraslab, zones A and B, respectively, relate to the plate boundary of the Indo-Australian and Eurasian plate collision zone. The M_w-9.0 earthquake of December 26, 2004 (number 1 in Figure 1) nucleated in zone A. In addition, the Sagaing fault zone striking north-south in central Myanmar, zone C, and the Sumatra fault zone striking northwest-southeast in Sumatra Island, zone E, are the major inland strike-slip faults in this region. According to Brown and Leicester (1933), an M_w-8.0 earthquake (number 2 in Figure 1) in zone C was created by the Sagaing fault zone on May 23, 1912, as were a number of other major earthquakes (Kundu and Gahalaut 2012). Zone D, the

Table 1 FMD coefficients (*a* and *b* values) and fractal dimensions (D_C) of 13 earthquake sources recognized in MLSEA

Name	EQ number	M_C	*a*	*b*	D_C
A: Sumatra-Andaman Interplate	414	4.7	5.98	0.768 ± 0.05	1.91 ± 0.01
B: Sumatra-Andaman Intraslab	560	4.7	6.58	0.877 ± 0.05	2.03 ± 0.02
C: Sagaing Fault Zone	101	4.7	5.8	0.864 ± 0.1	1.61 ± 0.02
D: Andaman Basin	87	4.3	4.51	0.611 ± 0.05	2.17 ± 0.03
E: Sumatra Fault Zone	139	4.8	4.75	0.606 ± 0.06	1.96 ± 0.01
F: Hsenwi-Nanting Fault Zones	48	4.8	6.02	1.01 ± 0.3	1.48 ± 0.01
G: Western Thailand	22	4.4	3.98	0.668 ± 0.2	N/A
H: Southern Thailand	9	N/A	N/A	N/A	N/A
I: Jinghong-Mengxing Fault Zones	84	4.2	4.87	0.712 ± 0.08	1.85 ± 0.01
J: Northern Thailand-Dein Bein Phu	62	4	4.72	0.732 ± 0.09	1.86 ± 0.04
K: Song Da-Song Ma Fault Zones	10	N/A	N/A	N/A	N/A
L: Xianshuihe Fault Zone	197	4.5	6.14	0.915 ± 0.09	1.80 ± 0.02
M: Red River Fault Zone	49	4.4	5.99	1.03 ± 0.1	1.48 ± 0.03

N/A, not applicable.

Andaman Basin off the coast of Andaman Sea, is occupied by transform fault systems consisting of the Andaman transform zone and Central Andaman rift in addition to the West Andaman and Seuliman faults (Cattin et al. 2009). Tectonically, zones C, D, and E include the plate boundary between the Burma and Sunda plates (Kundu and Gahalaut 2012).

Along the Thailand-Laos-Myanmar border, two strike-slip fault systems were detected. The northwest-southeast striking faults included in the Moei-Tongyi (Pailoplee et al. 2009) and Sri Sawat (Nuttee et al. 2005) fault zones are grouped into zone G. An earthquake of M_w-5.9 (number 3 in Figure 1) occurred in the Moei-Tongyi fault zone on February 17, 1975, whereas an M_w-5.6 earthquake (number 4 in Figure 1) occurred at the Sri Sawat fault zone on April 22, 1983 (Klaipongphan et al. 1991). In contrast, the northeast-southeast striking faults, the Ranong and Klong Marui fault zones, respectively, are delineated in the border between southernmost Myanmar and southern Thailand, which form zone H. An M_w-5.0 earthquake (number 5 in Figure 1) originated in this zone on October 8, 2006 (Yadav et al. 2012), at the northern end of the Ranong fault zone.

In northern Thailand, approximately north-south-trending grabens and their basin-bounding normal faults, such as the Lampang-Thoen (Charusiri et al. 2004), Phrae (Udchachon et al. 2005), and Mae Tha (Rhodes et al. 2004) fault zones, are classified as zone J in northern Thailand-Dein Bein Phu (Pailoplee and Choowong 2013). Most earthquakes nucleated in this area have been high-frequency, small-to-medium-sized earthquakes.

Along the southern China-Vietnam border, the northeast-southwest and northwest-southeast complex shear zones (Polachan et al. 1991) were grouped into the five zones of F, I, and K to M for the Hsenwi-Nanting, Jinghong-Mengxing, Song Da-Song Ma, Xianshuihe, and Red River fault zones, respectively. Instrumental earthquake records reveal that seismic activities in these zones are not quiescent.

Seismicity

The datasets used for this study are of the instrumentally recorded earthquakes and were provided by (i) the Incorporated Research Institutions for Seismology (IRIS) and (ii) the US National Earthquake Information Center (NEIC) earthquake catalogs. The combined data from these two sources yielded approximately 29,990 recorded earthquake events during the 50-year period of 1962 to 2013. These earthquake magnitudes ranged from 1.0 to 9.0 and were reported mostly in the body-wave magnitude scale (m_b). To homogenize the magnitude scale, earthquake events recorded in moment magnitude (M_w) and surface-wave magnitude (M_S) scales were converted to m_b, following the relationships proposed by Pailoplee et al. (2009). Both foreshocks and aftershocks, which are meaningless in seismotectonic investigations, were identified and removed by using the assumption reported by Gardner and Knopoff (1974). As a result, approximately 3,730 unique mainshock events remained in the database.

Thereafter, the Genetic Network Analysis System (GENAS) algorithm (Habermann 1987), implemented in the Z-MAP program (Wiemer 2001), was used to screen for any significant levels of bias from man-made seismicity variations in reporting and seismotectonic activities (Wyss 1991; Zuniga and Wiemer 1999). On the basis of the GENAS algorithm, 2,150 unique mainshock events with magnitudes of ≥4.0 m_b reported during the period 1974 to 2010 exhibited a smooth cumulative rate of change and thus formed the completeness catalog used here for the

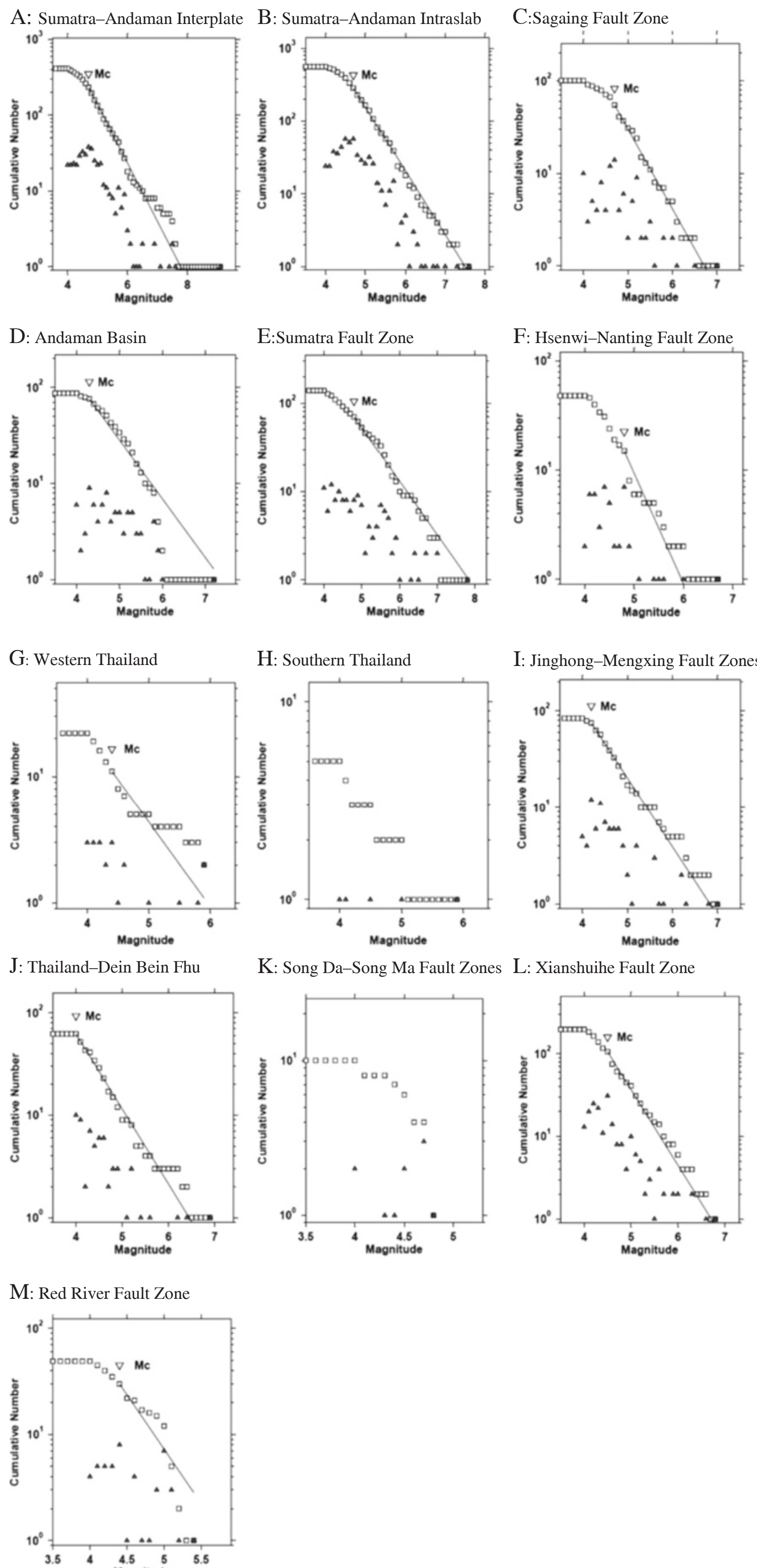

Figure 2 (See legend on next page.)

(See figure on previous page.)
Figure 2 Frequency-magnitude distribution (FMD) plots of the 13 seismic source zones (A to M). Triangles and squares represent the number and cumulative number of each individual magnitude level of earthquake, respectively. The lines represent the FMD linear regression fitted with the observed data. M_C is defined as the magnitude of completeness (Woessner and Wiemer 2005).

statistical seismicity investigation. The distribution of the completeness earthquakes is shown in Figure 1.

Results and discussions

Frequency-magnitude distribution

According to Gutenberg and Richter (1944), the FMD power law can be expressed as

$$\log(N) = a - bM \tag{1}$$

where N is the cumulative number of earthquakes with a magnitude $\geq M$. The a and b coefficient values vary in any specific time and space window. Seismotectonically, the a value indicates the entire seismicity level, and the b value relates to tectonic stress (Mogi 1967; Scholz 1968). Lower b values relate to higher levels of accumulated stress (Manakou and Tsapanos 2000).

Although Pailoplee and Choowong (2013) have previously plotted the FMDs and determined the coefficients for all seismic source zones in the MLSEA, the dataset used was not screened to exclude man-made seismicity artifacts. Therefore, to theoretically achieve more accurate results, the FMD a and b values were redetermined (Figure 2) along with the D_C values for these 13 zones of the MLSEA (Table 1).

Due to the lack of available earthquake data, the FMD plots of zones Hand K are unavailable. However, the calculated b values for the other zones were within the range of 0.61 to 1.03. The lowest b value was observed in zone E, whereas the highest b value was detected in zone M.

According to Bayrak and Bayrak (2012), the obtained b values can be categorized into four groups of $b < 0.7$, $0.7 \leq b < 0.8$, $0.8 \leq b < 0.9$, and $b \geq 0.9$. The variation in the b values in this study region, expressed as the four aforementioned category groups, is represented in Figure 3 by various colors. The highest b value group was observed at zones F, L, and M. With regard to the corresponding high a values of 5.99 to 6.14 (Table 1), this group is interpreted as a low-stress region due to frequent tension release through small earthquakes. The second group of b values (0.8 to 0.9) was detected at zones B and C, whereas b values of 0.7 to 0.8 were observed in zones A, I, and J. The b values of less than 0.7 were detected at zones D, E, and G. Regardless of the a value, these comparatively low b value regions may accumulate high tectonic stress levels.

Fractal dimension (D_C)

In this study, the D_C value was evaluated according to the correlation integral technique (Grassberger and Procaccia 1983) expressed as

$$C(r) = \frac{2}{N(N-1)} N(R < r) \tag{2}$$

where N is the number of earthquakes analyzed, and $N(R < r)$ is the number of event pairs separated by a distance $R < r$. If the distribution is fractal, the relation obtained will be the same as that in Equation 3 (Kagan and Knopoff 1980), which can be expressed as

$$C(r) \sim r^{(D_C)}. \tag{3}$$

Unlike the b value, the D_C value has not been reported previously for the MLSEA. Therefore, the D_C graphs of the 13 seismic source zones in the MLSEA were established (Figure 4). The slopes of the linear fit of graphs $\log(C(r))$-$\log(r)$ were the estimated D_C values (Table 1). Because of the statistical insufficiency of the available earthquake data, the D_C values for zones G, H, and K could not be evaluated.

The calculated D_C values varied between 1.48 and 2.17, with the lowest D_C values found at zones F and M. The highest D_C value, 2.17, was observed at zone D. From the definition of Tosi (1998), which states that the D_C value of seismogenically active sources ranges between 0 and 2, most of the MLSEA zones were interpreted as being seismically active.

The D_C values were divided into four groups of $D_C < 1.5$, $1.5 \leq D_C < 1.7$, $1.7 \leq D_C < 1.9$, and $D_C \geq 1.9$ (Bayrak and Bayrak 2012) and are mapped in Figure 5 by various colors. The highest D_C values were detected in zones A, B, D, and E. Second-level D_C values (1.7 to 1.9) were detected in zones I, J, and L; D_C values between 1.5 and 1.7 were observed only in zone C.

Empirically, a D_C value close to 1 or 2 signifies that the earthquake epicenters are homogeneously distributed over a line and two-dimensional (2-D) fault plane, respectively (Yadav et al. 2011). Therefore, most zones mentioned exhibit the near-plane characteristics of the seismogenic structures. Moreover, the lowest D_C values (<1.5), indicating an active linear fault system, were observed in zones F and M.

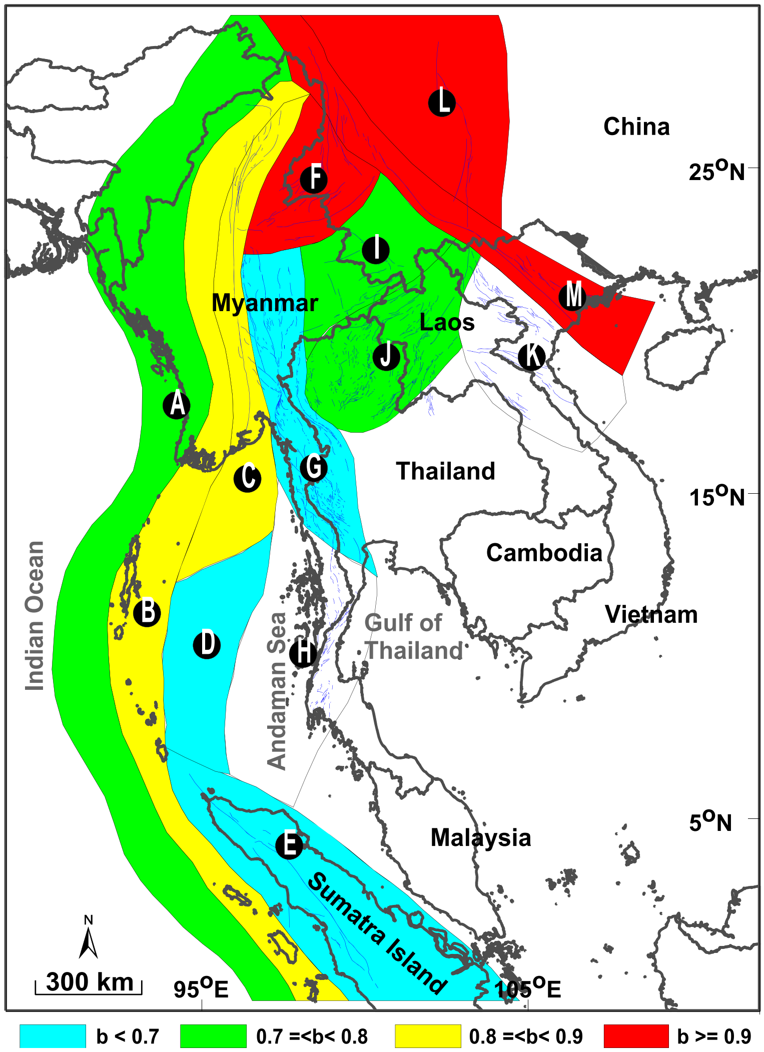

Figure 3 Map showing distributions of estimated *b* values for zones A to M proposed in MLSEA.

D_C/b relationship

The D_C/b ratio has been suggested as an effective indicator of seismic hazards (Bayrak and Bayrak 2011, 2012). Accordingly, in this study, the correlation between the D_C and b values was investigated according to that reported in previous works (Legrand 2002; Wyss et al. 2004; Mandal and Rastogi 2005; Bayrak and Bayrak 2012). On the basis of the obtained D_C and b values (Table 1), the empirical D_C/b relationship was calibrated as shown in Figure 6a and can be expressed as

$$D_c = 2.80–1.22b \tag{4}$$

Empirically, the D_C/b correlation can be either a positive or a negative regression. For example, positive regression was reported for the San Andreas fault in the USA, in addition to faults in India (Wyss et al. 2004; Yadav et al. 2012), whereas negative correlation was reported for fault zones in Japan, Turkey, and Iran (Hirata 1989; Öncel et al. 1996; Barton et al. 1999; Öncel and Wilson 2002; Poroohan and Teimournegad 2010).

For the MLSEA, the D_C/b relationship showed a distinct negative linear regression (Figure 6a), which implies increased accumulated stress and decreased earthquake clustering (Barton et al. 1999; Öncel and Wilson 2002). Therefore, in the MLSEA, zones D and E were defined as the highest stress regions, whereas zones F and M exhibited low-stress accumulations. Moreover, zones A, B, C, I, J, and L cluster in the middle of the graph with b values of approximately 0.71 to 0.92 and D_C values of approximately 1.61 to 2.03.

In addition, the relation between the D_C values and a/b ratios were investigated as per Bayrak and Bayrak (2012).

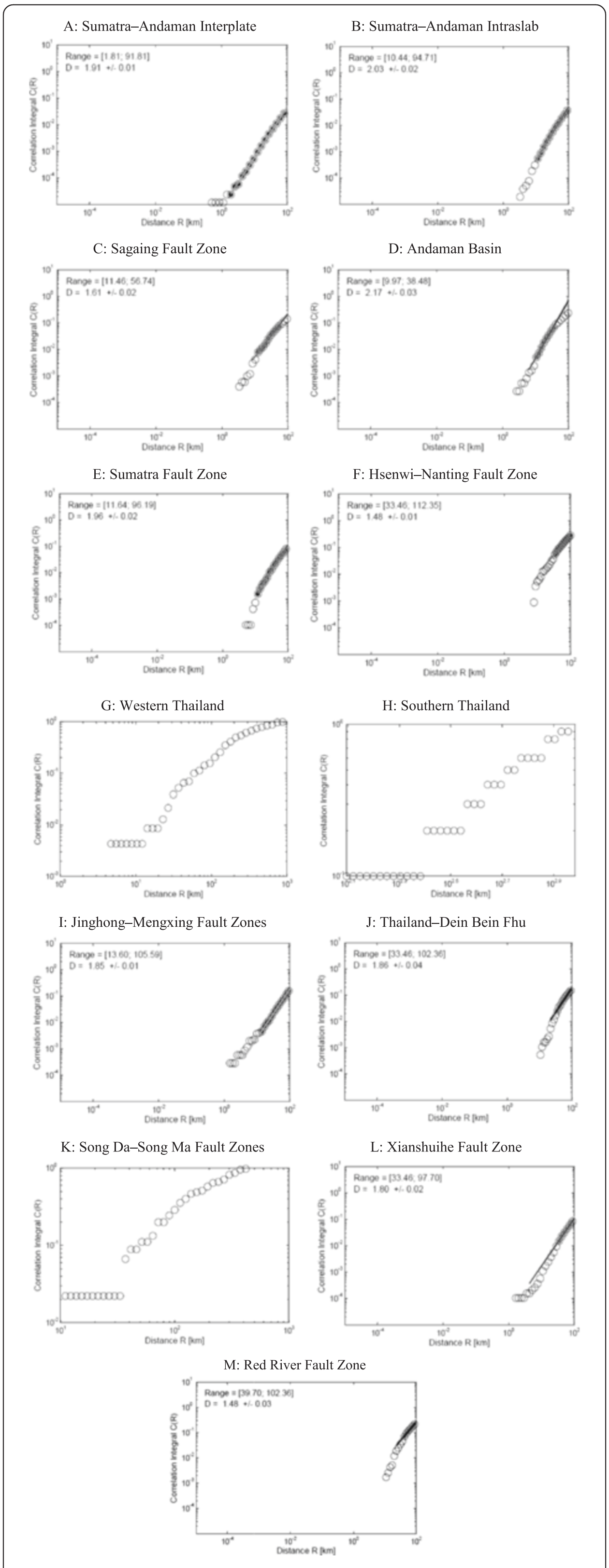

Figure 4 Graphs showing relationship between log(C(r)) and log(r) of earthquake data for 13 seismic source zones (A to M). The slopes of linear fit (solid black lines) are the fractal dimension (D_C).

The calibration (Figure 6b) revealed a positive correlation as

$$D_c = 0.27(a/b)\text{–}0.01 \quad (5)$$

A comparison of Figure 6a,b reveals that the distributions of both the D_C/b and D_C-(a/b) correlations were not significantly variant in terms of the data scatter. However, the D_C-(a/b) correlation showed a positive regression, whereas the D_C-b correlation showed a negative regression. Zones A and B of the interplate regime were moved from the middle group to the first group, which are of high a/b and D_C values. According to the entire seismicity rate, the a value for both zones was higher than that in the other zones. Although Bayrak and Bayrak (2012) mentioned that the D_C-(a/b) relationship was more reliable and effective than that of the D_C-b for indicating seismic hazards, both relationships in this study depicted an identical accuracy based on the R^2 values of 0.65 to 0.68. Therefore, both relationships between D_C-b and D_C-(a/b) could potentially reflect local seismicity and earthquake risk and can thus be useful in hazard studies, particularly in the MLSEA.

Conclusions

In this study, instrumental earthquake data recorded within the MLSEA were analyzed simultaneously in terms of the FMD b and the D_C values from 13 seismic source zones. The results revealed that regional variations in both the b and D_C values could imply local tectonic stress and hazard levels. According to the obtained D_C values, nearly all of the zones in the MLSEA are seismically active, and earthquakes are homogeneously distributed within the aerial fault plane. In addition, among the 13 seismic sources, zones A, B, D, and E showed comparatively low b and high D_C values. Conversely, zones F and M exhibited prominently high b and low D_C values.

Both the D_C-b and D_C-(a/b) relationships were calibrated in this study for the MLSEA region. Although the D_C/b correlation showed a negative regression, that for the D_C-(a/b) correlation was positive. In contrast to that reported by Bayrak and Bayrak (2012), which states that the D_C-(a/b) correlation represents seismotectonics more accurately than that of the D_C-b, in the present study of the MLSEA, both showed essentially similar correlations with R^2 values of 0.65 to 0.68. Therefore, both relationships can be used as an effective indicator of seismic hazards in the MLSEA region.

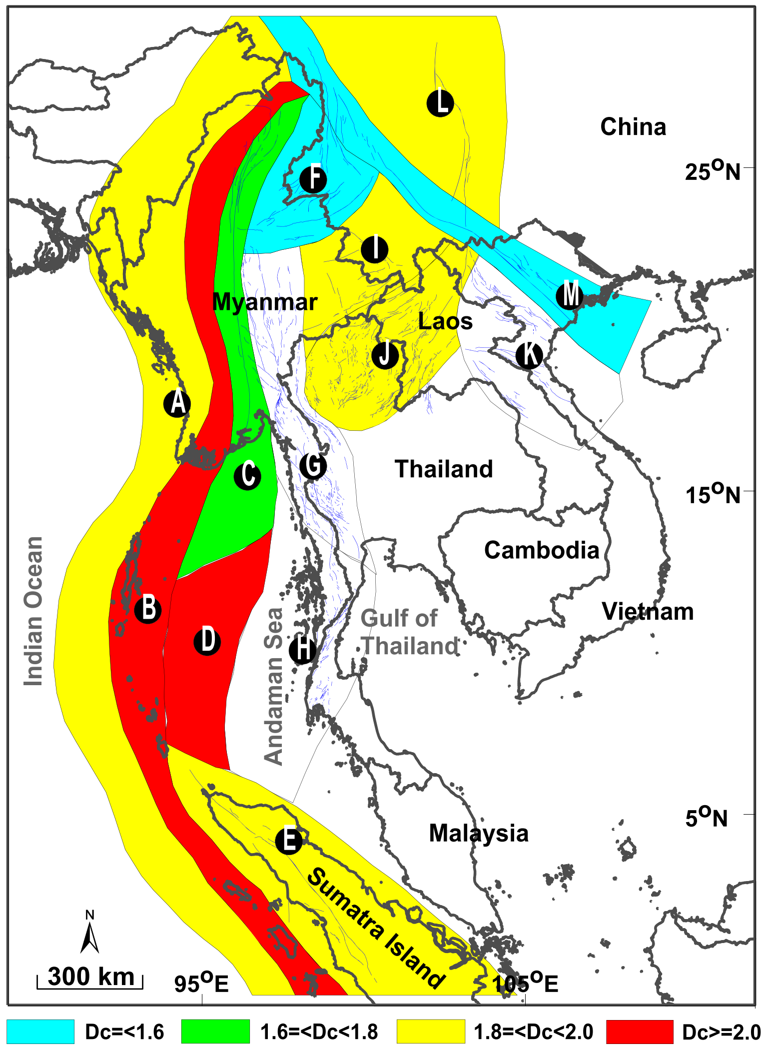

Figure 5 **Map showing distributions of estimated D_C values for zones A to M proposed in MLSEA.**

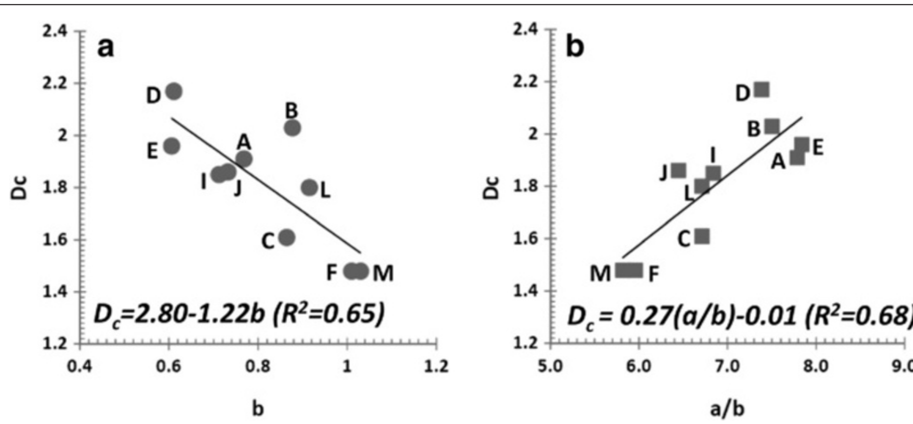

Figure 6 Empirical relationships. **(a)** Between the *b* and D_C values and **(b)** between the *a*/*b* ratios and D_C values for the 13 seismic source zones (A to M). The straight lines represent the linear regressions fitted with the observed data.

On the basis of both D_C/b and D_C-(a/b) relationships, it is interpreted tectonically that zones F and M are the low-stress zones that maybe safer against seismic hazards than other regions. Moreover, the interplate regimes of zones A, B, D, and E accumulated high levels of tectonic stress, which poses risks for generating large earthquakes in the future. Therefore, it is reasonable to suggest the introduction of seismic hazard warnings and the development of mitigation plans for the ASEAN community.

Competing interests
The authors declare that they have no competing interests.

Authors' contributions
SP carried out the seismicity investigations, performed the statistical analysis, and drafted the manuscript. MC participated in the design of the study and the sequence alignment. Both authors read and approved the final manuscript.

Acknowledgments
This research was jointly sponsored by the Ratchadapiseksomphot Endowment Fund of Chulalongkorn University (RES560530028CC) and the Thailand Research Fund (TRF) Grant for New Researchers. Additional thanks are extended to T. Pailoplee for the preparation of the draft manuscript. We thank the Publication Counseling Unit (PCU), Faculty of Science, and Chulalongkorn University for critical reviews and suggestions for improving the English. We also acknowledge the thoughtful comments and suggestions by Y. Ogawa (Editor in Chief), T. Okada, and anonymous reviewers, which significantly enhanced the quality of this manuscript.

Received: 14 January 2014 Accepted: 25 March 2014
Published: 9 April 2014

References
Barton DJ, Foulger GR, Henderson JR, Julian BR (1999) Frequency-magnitude statistics and spatial correlation dimensions of earthquakes at Long Valley Caldera, California. Geophys J Int 138:563–570
Bayrak Y, Bayrak E (2011) An evaluation of earthquake hazard potential for different regions in Western Anatolia using the historical and instrumental earthquake data. Pure Appl Geophys 169:1859–1873
Bayrak Y, Bayrak E (2012) Regional variations and correlations of Gutenberg–Richter parameters and fractal dimension for the different seismogenic zones in Western Anatolia. J Asian Earth Sci 58:98–107
Brown JC, Leicester P (1933) The Pyu earthquake of 3rd and 4th December, 1930 and subsequent Burma earthquakes up to January 1932. Memoirs Geolog Survey India 42(1):1–140
Cattin R, Chamot-Rooke N, Pubellier M, Rabaute A, Delescluse M, Vigny C, Fleitout L, Dubernet P (2009) Stress change and effective friction coefficient along the Sumatra-Andaman-Sagaing fault system after the 26 December 2004 (Mw = 9.2) and the 28 March 2005 (Mw = 8.7) earthquakes. Geochem Geophys Geosyst 10:Q03011
Charusiri P, Daorerk V, Choowong M, Muangnoicharoen N, Won-in K, Lumjuan A, Kosuwan S, Saithong P, Thonnarat P (2004) The study on the investigations of active faults in Changwat Kanchanaburi area, western Thailand. Department of Geology, Faculty of Science, Chulalongkorn University, Bangkok, Thailand, Technical report, p 119, in Thai with English abstract
Charusiri P, Choowong M, Charoentitirat T, Jankaew K, Chutakositkanon V, Kanjanapayont P (2005) Geological and physical effect evaluation in the tsunami damage area for restoration and warning system. Department of Geology, Faculty of Science, Chulalongkorn University, Bangkok, Thailand, Technical report, p 412, in Thai with English abstract
Gardner JK, Knopoff L (1974) Is the sequence of earthquakes in Southern California, with aftershocks removed, Poissonian? Bull Seismol Soc Am 64(1):363–367
Grassberger P, Procaccia I (1983) Measuring the strangeness of strange attractors. Physica D9:189–208
Gutenberg B, Richter CF (1944) Frequency of earthquakes in California. Bull Seismol Soc Am 34:185–188
Habermann RE (1987) Man-made changes of seismicity rates. Bull Seismol Soc Am 77:141–159
Hirata T (1989) Fractal dimension of fault system in Japan: fractal structure in rock fracture geometry at various scales. Pure Appl Geophys 131(1/2):157–170
Kagan YY, Knopoff L (1980) Spatial distribution of earthquakes: the two-point correlation function. Geophys J Roy Astron Soc 62:303–320
Klaipongphan S, Chakramanont V, Pinrode J, Chittrakarn P (1991) Geological and seismicity evaluation. Proceedings of the Second International Conference on Recent Advances in Geotechnical Earthquake Engineering and Soil Dynamics, St. Louis, Missouri, pp 1357–1363
Kundu B, Gahalaut VK (2012) Earthquake occurrence processes in the Indo-Burmese wedge and Sagaing fault regions. Tectonophysics 524–525:135–146
Legrand D (2002) Fractal dimensions of small, intermediate, and large earthquakes. Bull Seismol Soc Am 92:3318–3320
Manakou MV, Tsapanos TM (2000) Seismicity and seismic hazard parameters evaluation in the island of Crete and the surrounding area inferred from mixed data files. Tectonophysics 321:157–178
Mandal P, Rastogi BK (2005) Self-organized fractal seismicity and bvalue of aftershocks of the 2001 Bhuj earthquake in Kutch (India). Pure Appl Geophys 162:53–72
Mogi K (1967) Earthquakes and fractures. Tectonophysics 5(35–55):2005
Nutalaya P, Sodsri S, Arnold EP (1985) Series on seismology-volume II-Thailand. In: Arnold EP (ed) Technical report, Southeast Asia Association of Seismology and Earthquake Engineering, p 402
Nuttee R, Charusiri P, Takashima I, Kosuwan S (2005) Paleo-earthquakes along the southern segment of the Sri Sawat Fault, Kanchanaburi, Western Thailand: morphotectonic and TL-dating evidences, Proceedings of the International Conference on Geology, Geotechnology and Mineral Resources of Indochina, Khon Kaen, Thailand, 28–30 November 2005, pp 542–554
Öncel AO, Wilson T (2002) Space-time correlations of seismotectonic parameters and examples from Japan and Turkey preceding the Izmit earthquake. Bull Seismol Soc Am 92:339–350
Öncel AO, Main I, Alptekin Ö, Cowie P (1996) Temporal variations in the fractal properties of seismicity in the north Anatolian fault zone between 31°E and 41°E. Pure Appl Geophys 147:147–159
Pailoplee S, Choowong M (2013) Probabilities of earthquake occurrences in Mainland Southeast Asia. Arabian J Geosci 6:4993–5006
Pailoplee S, Sugiyama Y, Charusiri P (2009) Deterministic and probabilistic seismic hazard analyses in Thailand and adjacent areas using active fault data. Earth Planets Space 61:1313–1325
Pailoplee S, Channarong P, Chutakositkanon V (2013) Earthquake activities in the Thailand-Laos-Myanmar border region: a statistical approach. Terr Atmos Ocean Sci 24(Part II):721–730
Polachan S, Pradidtan S, Tongtaow C, Janmaha S, Intrawijitr K, Sangsuwan C (1991) Development of Cenozoic basins in Thailand. Mar Petrol Geol 8:84–97
Poroohan N, Teimournegad K (2010) An analysis of correlations of seismotectonic parameter and fractal dimension preceding Roudbar-Tarom earthquake (northwest of Iran). Int Conf Geology Seismology:148–154
Rhodes BP, Perez R, Lamjuan A, Kosuwan S (2004) Kinematics and tectonic implications of the Mae Kuang Fault, northern Thailand. J Asian Earth Sci 24(1):79–89
Scholz CH (1968) The frequency–magnitude relation of microfracturing in rock and its relation to earthquakes. Bull Seismol Soc Am 58:399–415
Tosi P (1998) Seismogenic structure behavior revealed by spatial clustering of seismicity in the Umbria-Marche Region (central Italy). Ann Geophys 41:215–224
Udchachon M, Charusiri P, Daorerk V, Won-in K, Takashima I (2005) Paleo-seismic studies along the southeastern portion of the Phrae Basin, Northern Thailand, Proceedings of the International Conference on Geology, Geotechnology and Mineral Resources of Indochina, Khon Kaen, Thailand, 28–30 November 2005, pp 511–519
Wiemer S (2001) A software package to analyze seismicity: ZMAP. Seismol Res 72:373–382
Woessner J, Wiemer S (2005) Assessing the quality of earthquake catalogues: estimating the magnitude of completeness and its uncertainty. Bull Seismol Soc Am 95(2):684–698
Wyss M (1991) Reporting history of the central Aleutians seismograph network and the quiescence preceding the 1986 Andreanof Island earthquake. Bull Seismol Soc Am 81:1231–1254
Wyss M, Sammis CG, Nadeau RM, Wiemer S (2004) Fractal dimension and b-value on creeping and locked patches of the San Andreas fault near Parkfield, California. Bull Seismol Soc Am 94:410–421

Yadav RBS, Papadimitriou EE, Karakostas VG, Rastogi BK, Shanker D, Chopra S, Singh AP, Kumar S (2011) The 2007 Talala, Saurashtra, western India earthquake sequence. Tectonic implications and seismicity triggering. J Asian Earth Sci 40(1):303–314

Yadav RBS, Gahalaut VK, Chopra S, Shan B (2012) Tectonic implications and seismicity triggering during the 2008 Baluchistan, Pakistan earthquake sequence. J Asian Earth Sci 45(2):167–178

Zuniga FR, Wiemer S (1999) Seismicity patterns: are they always related to natural causes? Pageoph 155:713–726

doi:10.1186/1880-5981-66-8
Cite this article as: Pailoplee and Choowong: **Earthquake frequency-magnitude distribution and fractal dimension in mainland Southeast Asia.** *Earth, Planets and Space* 2014 **66**:8.